BMC Geriatrics

RESEARCH

Open Access

White matter structure and derived network properties are used to predict the progression from mild cognitive impairment of older adults to Alzheimer's disease

Jiaxuan Peng[1,2†], Guangying Zheng[1,2†], Mengmeng Hu[1], Zihan Zhang[1,2], Zhongyu Yuan[1,2], Yuyun Xu[1], Yuan Shao[1], Yang Zhang[1], Xiaojun Sun[1], Lu Han[1,2], Xiaokai Gu[3], Zhenyu Shu[1*] and for the Alzheimer's Disease Neuroimaging Initiative

Abstract

Objective To identify white matter fiber injury and network changes that may lead to mild cognitive impairment (MCI) progression, then a joint model was constructed based on neuropsychological scales to predict high-risk individuals for Alzheimer's disease (AD) progression among older adults with MCI.

Methods A total of 173 MCI patients were included from the Alzheimer's Disease Neuroimaging Initiative(ADNI) database and randomly divided into training and testing cohorts. Forty-five progressed to AD during a 4-year follow-up period. Diffusion tensor imaging (DTI) techniques extracted relevant DTI quantitative features for each patient. In addition, brain networks were constructed based on white matter fiber bundles to extract network property features. Ensemble dimensionality reduction was applied to reduce both DTI quantitative features and network features from the training cohort, and machine learning algorithms were added to construct white matter signature. In addition, 52 patients from the National Alzheimer's Coordinating Center (NACC) database were used for external validation of white matter signature. A joint model was subsequently generated by combining with scale scores, and its performance was evaluated using data from the testing cohort.

Results Based on multivariate logistic regression, clinical dementia rating and Alzheimer's disease assessment scales (CDRS and ADAS, respectively) were selected as independent predictive factors. A joint model was constructed in combination with the white matter signature. The AUC, sensitivity, and specificity in the training cohort were 0.938, 0.937, and 0.91, respectively, and the AUC, sensitivity, and specificity in the test cohort were 0.905, 0.923, and 0.872, respectively. The Delong test showed a statistically significant difference between the joint model and CDRS or ADAS scores ($P < 0.05$), yet no significant difference between the joint model and the white matter signature ($P = 0.341$).

Conclusion The present results demonstrate that a joint model combining neuropsychological scales can be constructed by using machine learning and DTI technology to identify MCI patients who are at high-risk of progressing to AD.

Keywords Diffusion Tensor Imaging, White matter microstructure, Mild Cognitive Impairment, Alzheimer's Disease, Machine learning

†Jiaxuan Peng and Guangying Zheng contributed equally to this work.

*Correspondence:
Zhenyu Shu
cooljuty@hotmail.com
Full list of author information is available at the end of the article

Alzheimer's disease (AD) is a neurodegenerative disease that is progressive and highly disabling among older adults. Currently, there are no effective drugs that can significantly slow or cure the progression of AD [1]. Mild cognitive impairment (MCI) manifests in the precursor stage of AD, and approximately 10–12% of MCI patients progress to AD each year [2]. Early intervention during the MCI stage may potentially slow disease progression or maintain lifelong stability [3, 4]. Therefore, identifying MCI populations at high risk of progressing to AD is particularly important.

Over the past three decades, greater use of magnetic resonance imaging (MRI) has demonstrated that white matter is essential to subcortical structures. White matter is also closely related to cognitive function [5]. In particular, DTI technology has provided greater detail regarding the microstructure of white matter by evaluating the diffusion of water molecules along myelinated nerve fibers. Consequently, DTI quantitative parameters such as fractional anisotropy (FA) and mean diffusivity (MD)are often used to quantify the degree of water molecule diffusion within white matter [6, 7]. DTI technology has shown that the structural integrity of brain white matter in individuals carrying genetic mutations associated with AD is lower than that in non-carriers, and it also indicates that early pathological changes are associated with AD [8]. However, neither FA nor MD can generate specific information regarding possible roles for axonal, myelin, or other pathology [9]. Therefore, relying solely on routine DTI parameters may not be sufficient for fully characterizing the impact of white matter neuropathology on cognitive function.

White matter appears to mediate a transfer of information within distributed neural networks. Accordingly, damage that primarily affects white matter most prominently results in cognitive slowing [10]. In addition, AD is characterized by the deposition of amyloid-beta and tau proteins in the brain, which reduces neural activity and disrupts communication between various brain regions. Therefore, AD may lead to abnormal connections between different brain regions. Graph theory network analysis can be used to construct brain networks by regarding the brain as a small world, and relevant network features can be extracted [11, 12]. Subsequently, features of white matter brain networks can be combined with DTI features, which reflect structural changes in white matter. This approach may be advantageous in assessing heterogeneous information concerning MCI progression. However, the numerous redundant features involved require a precise and reliable method to select these features further and facilitate MCI progression studies.

As a branch of artificial intelligence, machine learning can directly extract the most predictive features from labeled data with minimal human intervention [13]. Machine learning has been established as a more robust approach to extract reliable predictors and automatically classifying different AD phenotypes [14]. Therefore, we hypothesize that combining fiber bundle features of white matter with their derived network properties features using emerging machine learning-based analysis methods can sensitively detect specific white matter changes in the early stages of preclinical AD. Moreover, these changes may accurately predict the progression of MCI to dementia.

Therefore, the primary aim of this study is to identify fiber bundle injuries and corresponding changes in white matter networks that may lead to disease progression in MCI patients. Secondly, we considered these features in combination with clinical features to generate a joint model to predict a high-risk population of MCI patients who are likely to progress to AD.

Demographic and clinical scale assessments

Data included in this study were obtained from the Alzheimer's Disease Neuroimaging Initiative (ADNI) website (https://adni.loni.usc.edu/), specifically from the ADNI-2 and ADNI-GO datasets and the National Alzheimer's Coordinating Center (NACC) databases (https://naccdata.org). Ethical review information regarding ADNI and NACC data is available on the website. A total of 173 patients with a baseline diagnosis of MCI from the ADNI database were included in the present study. Forty-five of these patients progressed to AD during a 4-year follow-up period and were classified as progression cases. The remaining 128 patients were classified as stable cases. Exclusion criteria include: DTI image quality is poor or the image cannot extract relevant features; The patient's follow-up examination time has not reached four years; Lack of evaluation of APOE4 and various neuropsychological scales; The patient progressed to AD but recovered to MCI within four years. Specific demographic information can be found in supplementary materials. Clinical data were collected, which included neuropsychological cognitive assessment scales information obtained from the Mini-Mental State Examination (MMSE), clinical dementia rating (CDR) [15], and Alzheimer's Disease Assessment Scale (ADAS), as well as demographic data such as age, gender, education level, APOE4, and conversion time. In this study, we randomly divided 173 study subjects into a training cohort ($n=121$) and a testing cohort ($n=52$) in a 7:3 ratio, the training set was used to construct a model, and the test set was used to validate the reliability of the model. In addition, the 52 patients collected from the National Alzheimer's

Coordinating Center (NACC) database (https://naccdata.org) were used as an external validation set, of which 15 patients progressed to AD during a 4-year follow-up period. They were classified as progression cases, while the remaining 37 patients were classified as stable cases; in addition, NACC database lacks clinical information on APOE4 and ADAS scales.

Data preprocessing and feature extraction

Initially, the FMRIB's Diffusion Toolbox and DTIFit tools in FSL software (https://fsl.fmrib.ox.ac.uk) were used for DTI images preprocessing, including format conversion, data quality detection, head movement, eddy current, and gradient direction correction, skull removal, obtaining brain masks, calculating tensors to obtain FA, MD, axial diffusion (rAD), and radial diffusion (RD) parameter maps. Detailed information regarding the processing steps applied can be found in the supplementary materials section. Next, the JHU ICBM-DTI-81 white matter labels atlas was used to extract DTI general parameters [16, 17]. This atlas included forty-eight fiber bundles, we calculated diffusion tensor parameters for a single fiber bundle for each participant, including FA, MD, rAD, and RD values. A total of 192 features reflecting water molecule anisotropy for each patient were extracted. The information about the white matter label atlas and the acquisition of corresponding white matter features can be found in the supplementary materials.

DSI-studio software (https://dsi-studio.labsolver.org/) was used to construct the DTI network. Specifically, a deterministic fiber tracking algorithm was applied with an enhanced tracking strategy to improve reproducibility. Details regarding the parameters used for fiber tracking with DSI-studio can be found in the supplementary materials section. The AAL2 atlas was used as a template, with specific brain regions identified as nodes. FA was the edge metric between the nodes, and it was used to construct a corresponding brain network matrix and to calculate network features. In total, 960 features reflecting changes in the topological properties of the DTI brain network were extracted. Names of the specific features are provided in the supplementary materials section.

Feature dimensionality reduction

Dimensionality reduction methods were used to perform feature dimensionality reduction on the DTI feature set and the white matter network feature set in the training cohort. Considering the large number of feature sets and small sample sizes extracted in this study, we used the ensemble dimensionality reduction method for feature selection to ensure that the most representative features can be obtained. The ensemble methods applied included variance analysis, Max-Relevance and Min-Redundancy (mRMR), Least Absolute Shrinkage and Selection Operator (LASSO), and Gradient Boosting Decision Tree (GBDT) dimensionality reduction methods. Since feature dimensionality reduction based solely on statistics may retain meaningless features, resulting in overfitting of constructed signature, we conducted logistic regression analysis on the remaining features of dimensionality reduction in this study, screened out independent predictive features reflecting MCI progression, and ultimately constructed the white signature based on the remaining features. Multiple logistic regression was applied to select significant features for model construction based on the remaining features of the two feature sets. Detailed steps regarding the dimensionality reduction performed are available in the supplementary materials section.

Construction of white matter signature

Machine learning algorithms constructed a white matter signature based on the selected features. Five machine learning classifiers were used: Support vector machine (SVM), Naive Bayes (NB), Decision Tree (DT), Random Forest (RF), and K-nearest neighbors (KNN). To avoid reporting biased results and limit overfitting, the machine learning algorithm uses a cross-validation program in the training cohort, including an external loop randomly dividing the training cohort ($n=121$) into training subgroups and testing subgroups. A total of 50 random splits are used to evaluate the classification performance, and the difference between the 50 reconstructions lies in the division of the training and test subgroups. The other is a fivefold cross-validation internal loop for optimizing the algorithm's hyperparameters to training subgroups. Cross-validation was repeated five times, once for each subsample, and the results of averaging five times yielded a single test value. The hyperparameter corresponding to the best performance test value is used to construct the large model in the outer loop. Finally, relative standard deviation (RSD) was used to quantify the performance and stability of the five machine learning algorithms. A minimum RSD value was selected as the optimal model construction method. RSD represents the absolute value of the coefficient of variation and is usually expressed as a percentage. The details of the calculation formula can be found in the supplementary material.

A correlation analysis was conducted to ascertain the reliability of the white matter signature and elucidate the potential mechanisms of their prediction. We investigated the association between features used to construct joint models and neuropsychological scales. Briefly, the white matter signature output was a binary prediction of disease progression in individuals with MCI, defined as stable or progressive. Details regarding the machine

learning aspect that was applied are provided in the supplemental materials section.

Construction and performance evaluation of the prediction model

Based on the identified white matter signature, the backward stepwise selection method with a stopping rule based on the Akaike information criterion (AIC) was used to select potential clinical predictive factors in the training cohort for constructing a joint prediction model using logistic regression [18]. The performance of the model generated was validated using data from the testing cohort. In addition, the Delong test was used to verify the diagnostic efficacy difference between the joint model and other predictive factors. The Hosmer–Lemeshow test was applied to analyze the goodness of fit for the joint model, and the calibration curve was used to assess consistency between predicted and actual MCI progression. A decision curve analysis was performed to evaluate the clinical net benefit of the joint model. A prognostic index (PI) value was calculated for each subject using the joint model to assess the clinical efficacy of the joint model. The ROC curve Youden index threshold corresponding to the optimal critical value was used as the classification point. All cases from the training and testing cohorts in the study were divided into a progression or stable subgroup according to their PI values, respectively. Kaplan–Meier survival curve analysis was also performed based on the ranking of the PI values obtained and was employed to examine differences in MCI conversion rates during different periods. A flow chart of the research process performed is presented in Fig. 1.

Statistical analysis

All statistical analyses were performed using SPSS software (version 17.0, IBM, Armonk, NY, USA) and R software (version 3.5.0). The SPSS software was used to study the correlation between screened DTI features and network features, and neuropsychological scales, as well as to screen independent predictive factors and construct joint model. R software was used in feature dimensionality reduction, white matter biomarker construction, and

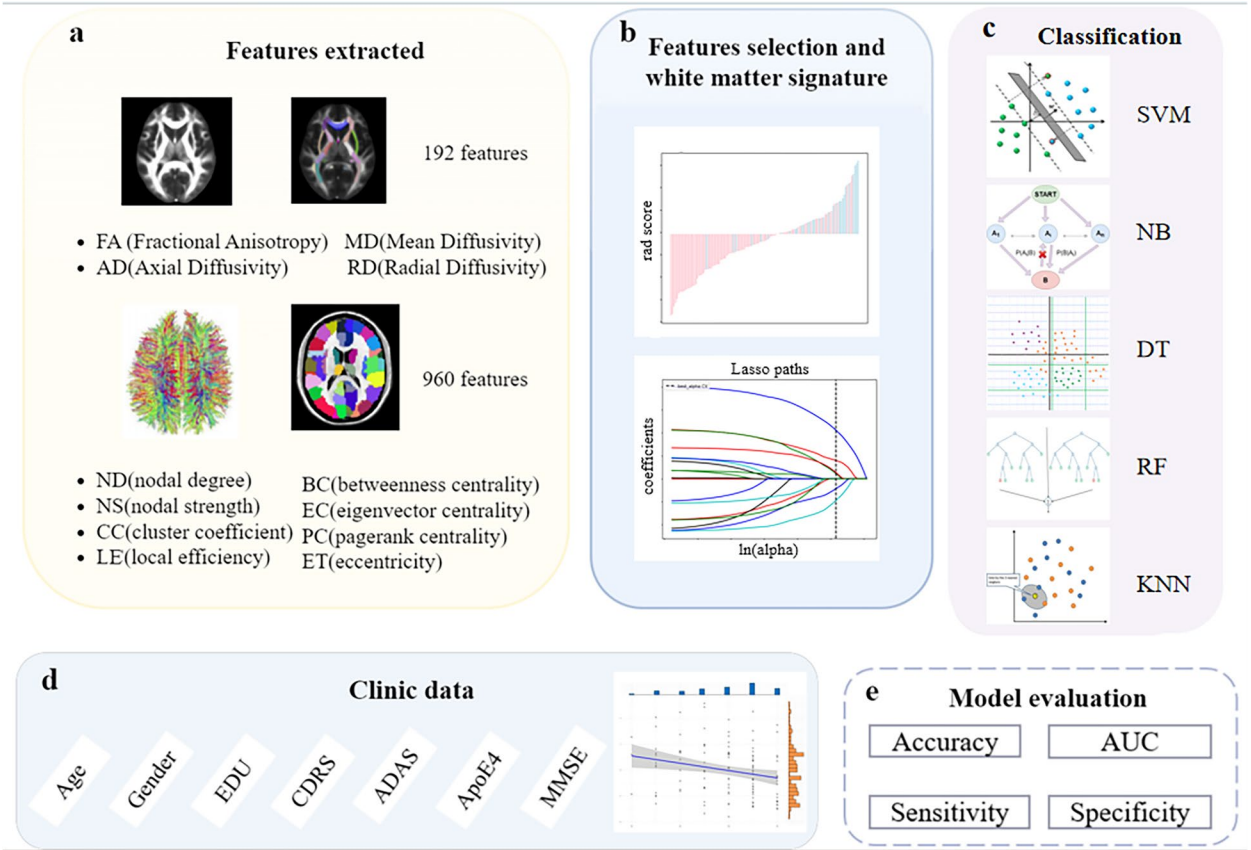

Fig. 1 Research flow chart. After extracting relevant DTI attribute features and white matter structure network features (**A**), an ensemble dimensionality reduction method is used for dimensionality reduction (**B**). Then, different machine learning methods are used to construct a white matter signature (**C**). Finally, a joint model was built based on this signature combined with clinical features (**D**), and the model is validated and evaluated (**E**)

Table 1 Comparative analysis of clinical data between MCI stable and progression subgroups

Characteristics		ADNI						NACC		
		Training set ($n=121$)			Test set ($n=52$)			Validation set ($n=52$)		
		MCI stable ($n=89$)	MCI progression ($n=32$)	*P* value	MCI stable ($n=39$)	MCI progression ($n=13$)	*P* value	MCI stable ($n=37$)	MCI progression ($n=15$)	*P* value
Gender(n, %)	Male	55 (61.80%)	18 (56.25%)	0.582	23(58.97%)	7 (53.85%)	0.746	23(62.16%)	11(73.33%)	0.443
	Female	34 (38.20%)	14 (43.75%)		16 (41.03%)	6 (46.15%)		14(37.84%)	4(26.67%)	
Age(year), mean(SD)		71.97 ± 7.40	74.89 ± 6.65	0.051	72.53 ± 8.4	67.04 ± 9.13	0.051	72.81 ± 5.74	75.40 ± 7.93	0.194
Education, mean(SD)		15.82 ± 2.65	16.03 ± 2.79	0.704	16.77 ± 2.21	15.54 ± 2.76	0.108	16.11 ± 2.50	14.53 ± 3.16	0.063
ADAS, mean(SD)		8.40 ± 3.55	13.11 ± 5.44	< 0.001*	9.17 ± 4.88	13.05 ± 3.92	0.012*	NA	NA	NA
CDR, mean(SD)		1.21 ± 0.73	1.80 ± 0.75	0.001*	1.19 ± 0.76	1.92 ± 0.76	0.004*	0.69 ± 0.85	2.23 ± 1.19	< 0.001
APOE4 (n, %)	negative	48 (53.93%)	8 (25.00%)	0.005*	22(56.41%)	5 (38.46%)	0.262	NA	NA	NA
	positive	41 (46.07%)	24 (75.00%)		17(43.59%)	8 (61.54%)		NA	NA	

CDRS Clinical Dementia Rating Scale, *ADAS* Alzheimer's Disease Assessment Scale, *MMSE* Mini-Mental State Examination, *NA* Not available because the variable is not included in the NACC database

related machine learning research. The normality of the continuous variables was analyzed by applying the Shapiro–Wilk test. Continuous variables are expressed as mean ± SD, while categorical variables are presented as frequency and percentage. The T-test, Mann–Whitney U-test, and Chi-square test were used to compare differences in categorical or continuous variables, with $P < 0.05$ indicating statistical significance.

Results

Comparisons of clinical factors

In the training and testing group, significant differences were observed among the CDRS, ADAS, and MMSE scores in the two groups ($P < 0.05$). In the training group, there was a statistical difference in APOE4 ($P < 0.05$); in the test group, there was no statistical difference. In the validation set, there are significant differences in CDRS between the progression and stable MCI groups (Table 1).

Construction of a white matter signature

After applying an ensemble dimensionality reduction method, 18 features were selected from the training cohort. These included 12 white matter network features and 6 DTI quantitative features (Fig. 2). After performing multiple logistic regressions on these 18 features, 10 features were selected to represent differences in brain white matter attributes between the MCI progression and stable groups. These included six brain network features and four DTI features (TableS4 and Fig. 3, respectively). Based on these ten features, a white matter signature was constructed using the SVM algorithm, with a minimum RSD value of 6.47 (Table 2). The white matter signature had an AUC value of 0.919, and its sensitivity and specificity values were 0.781 and 0.944 in the training dataset. The AUC, sensitivity, and specificity in the test group were 0.905, 0.923, and 0.872, respectively. The AUC, sensitivity, and specificity in the validation group were 0.905, 0.667, and 0.946, respectively(Fig. 5C). In addition, correlations between these ten features and clinically relevant features, including APOE4, CDRS, ADAS, and MMSE scores, were analyzed. Negative correlations were observed between betweenness_centrality_Precentral_R and CDR ($r = -0.203$, $P = 0.025$), and between pagerank_centrality_Temporal_Inf_R, betweenness_centrality_Precentral_R, and ADAS scores ($r = -0.241$, -0.27; $P = 0.008$, 0.003). Furthermore, MD_Cingulum (hippocampus) R was found to negatively correlate with MMSE scores ($r = -0.233$, $P = 0.001$), while FA_Uncinate fasciculus L positively correlated with MMSE scores ($r = 0.246$, $P = 0.007$) (Fig. 4).

Construction of prediction model

A joint model was constructed using CDR and ADAS scores (which were selected as independent predictors based on multiple logistic regression) combined with an SVM white matter signature (Table 3). The AUC value of the joint model based on ten-fold cross-validation was 0.938, with sensitivity and specificity values of 0.937 and 0.91, respectively. In the test group, the AUC, sensitivity, and specificity of the joint model were 0.937, 0.923, and 0.897, respectively. In both the training and test group, The Delong test demonstrated that the joint model exhibited a statistically significant difference compared to the CDRS and ADAS scores ($P < 0.05$) in the training and testing group. In contrast, there was no statistically significant difference between the joint model and the white matter signature ($P = 0.341$) (Fig. 5A, B)in the training and testing group. The optimal cut-off point corresponding to the Youden index on the ROC curve of the joint model was 0.2474, which was used to classify the data into low-risk and high-risk groups. The Log-rank test showed a significant difference between the survival curves of the low-risk and high-risk groups in the training and testing group ($P < 0.001$)(Fig. 6A, B).

Discussion

This study proposed a classification method based on white matter-derived structural and network properties to identify high-risk individuals for MCI progression. The white matter signature constructed using an SVM classifier achieved a diagnostic accuracy of 0.919 for identifying MCI progression to AD. This result demonstrates the superiority of machine learning in integrating different feature attributes. Moreover, the joint model constructed using white matter signature and multiple cognitive scale scores based on ten-fold cross-validation demonstrated good robustness and higher sensitivity and accuracy, indicating the potential value of a joint model approach for identifying MCI progression.

We observed that FA has more advantages than other DTI values, which is consistent with the results of many studies [19]. Furthermore, the uncinate fasciculus, fornix, middle cerebellar peduncle (MCP), and hippocampal cingulum bundle (HCB) have been shown to predict the conversion from MCI to AD [20, 21]. These neural fiber bundles often connect to gray matter structures associated with memory function. Meanwhile, the hippocampus and amygdala have been identified as imaging biomarkers for early identification of AD [22, 23]. In this study, the microstructure of the fornix has been associated with memory performance, which is consistent with the research of Rudebecket al. [24] and Fletcher et al. [25]. The MCP is part of the vermis of the cerebellum, which

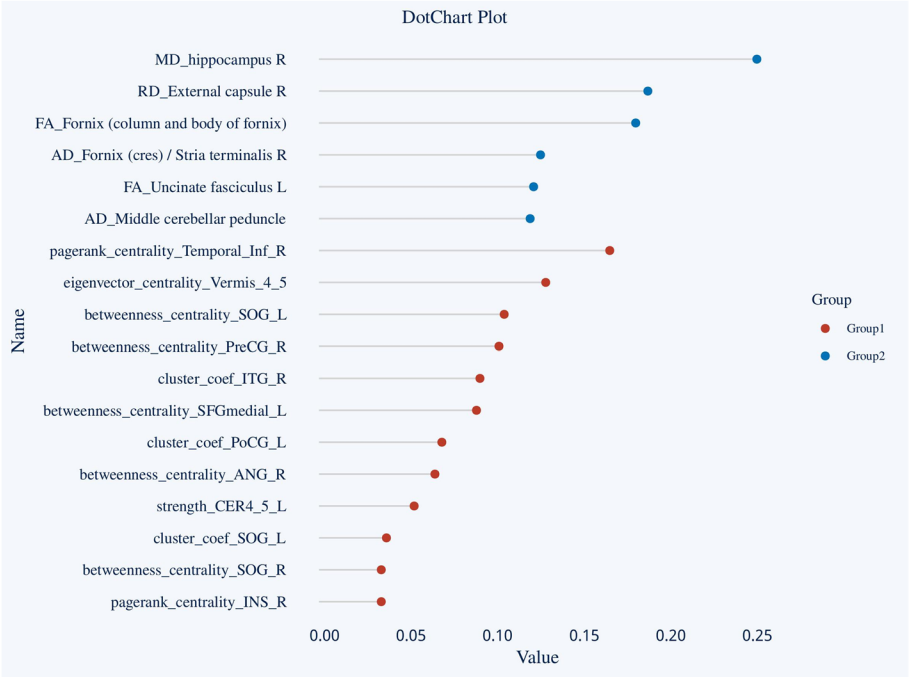

Fig. 2 Slide dot-chart of features after integrated dimension reduction. Group 1 represents the brain network features, while Group 2 represents the DTI features. The horizontal axis indicates the weights of each feature

has often been neglected in previous studies. Gupta et al. [26] observed that the high metabolism of the cerebellum is related to an increase in betweenness centrality (BC), indicating that the cerebellum plays an essential role in brain connectivity changes during AD. In addition, The right hippocampal cingulum bundle is consistent with the results of Stone et al. [27]. However, their model was based on selected specific white matter bundle regions and only achieved an accuracy of 0.75. In comparison, an accuracy of 0.938 was achieved in the present study, which may represent a benefit of the contributions from the white matter networks. Other studies have shown that the corpus callosum, inferior longitudinal fasciculus, and internal capsule are the best predictors of MCI to AD conversion [28]. Although the fiber bundles with lesions that were previously considered differ among many studies, the white matter lesions related to AD progression consistently tend to involve white matter fibers that are closely related to the AD-damaged cortex, such as the temporal and parietal lobes.

Traditionally, individual fiber bundle features have been analyzed. However, this approach does not adequately reflect the separation and integration between different brain regions while evaluating anisotropy scores. The human brain network has small-world properties [12, 29]. The BC of the Frontal_Sup_Medial_L, Precentral_R, and Angular_R obtained from the DTI white matter network we constructed can serve as imaging indicators for an auxiliary diagnosis of AD. Among them, BC is a local node index that can quantify the amount of information that may pass through any brain area. However, BC may also exaggerate node contributions. We observed that eigenvector centrality and PageRank also affect disease progression. Zhang et al. have used graph theory and machine learning methods to distinguish MCInc from MCIc by combining sMRI and rs-fMRI indicators [30]. With this strategy, an accuracy of 89.9% was achieved. Hojjatiet al. predicted MCI progression with only rs-fMRI, with an accuracy of 91.4% [31]. When we combined both DTI and brain network features, better predictive performance of the resulting model was achieved compared with these previously reported models. This result might be due to differences in sequence selection and feature dimensionality reduction. However, although there are differences in the methods used to extract features, a high degree of similarity still exists in the final abnormal brain regions (e.g., frontal lobe, temporal lobe, thalamus, right precentral gyrus, and angular gyrus). We hypothesize that the probability of information transmission between these brain regions is high, and the corresponding brain regions are accordingly active. Thus, when the brain regions activated during attention tasks and memory extraction are damaged, it is possible that intrinsic differences already exist.

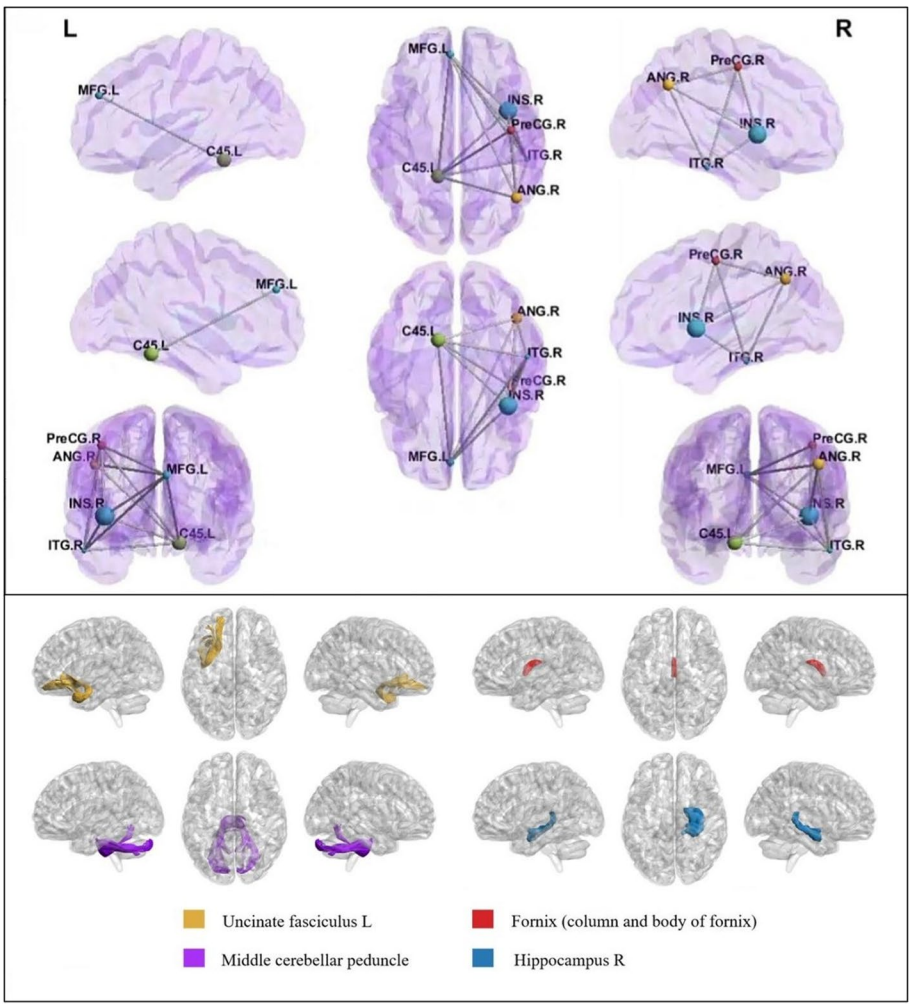

Fig. 3 Brain networks feature and DTI feature visualization. **A** shows a brain network diagram of white matter structure, where each line represents the network features between two brain regions (abbreviations can be found in auxiliary materials). **B** shows the position of white matter fiber bundles corresponding to DTI features

Table 2 Predictive performances of different machine learning methods

Model	Mean value	SD	RSD (%)
Bayes	0.8195	0.0838	10.22
Forest	0.7581	0.1096	14.45
KNN	0.8204	0.0712	8.67
SVM	0.8998	0.0582	6.47
DT	0.6529	0.0958	14.67

SD Standard deviation, *RSD* Relative standard deviation, *KNN* K-nearest neighbor, *SVM* Support vector machine, *DT* Decision tree

Zhou et al. used DTI imaging to track fibers related to the hippocampus-temporal lobe and thalamus [32]. They observed that degenerative fibers detected by DTI indices, especially those associated with the hippocampus-temporal lobe, significantly correlated with cognitive scores compared to standard fibers. Similarly, the results of the present study also exhibit a correlation between the hippocampal cingulum and MMSE scores. This result is consistent with theirs. Additionally, it is worth noting that Zhou et al. only selected regions of interest that exhibited a high level of resting-state functional connectivity with the hippocampus as seeds to track fibers. In the present study, we expanded the scope to include the entire brain, and anisotropy values corresponding to specific fiber bundles were specified. For example, the FA value of the left uncinate fasciculus positively correlated with MMSE scores. This result indicates that better integrity of the left uncinate fasciculus correlates with better cognitive performance. Overall, our results demonstrate that the cognitive ability of MCI and AD patients is affected by

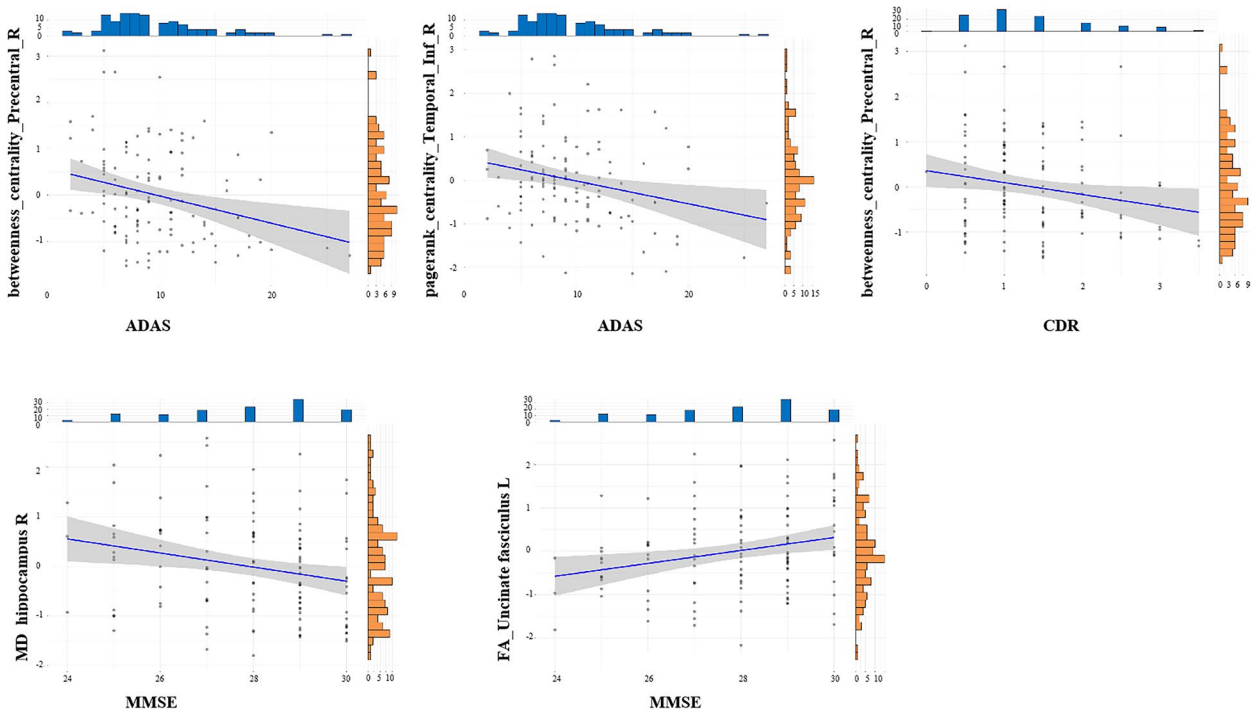

Fig. 4 Correlation analysis between significantly distinguishable important features and each independent predictor. The blue bars represent the histogram distribution of cognitive rating scales such as CDRS, ADAS, and MMSE, and the orange bars represent the histogram distribution of the final selected important DTI and network features

Table 3 Independent predictors of MCI status in univariate and multivariate logistic regression analysis

Variable	Univariate logistic regression		Multivariate logistic regression	
	OR (95%CI)	*P* value	OR (95%CI)	*P* value
Gender	2.319 (0.748,7.188)	0.145	NA	NA
APOE4	4.645 (1.313, 16.431)	0.017*	NA	NA
Age (y)	1.097 (1.014, 1.186)	0.021*	NA	NA
Education	1.052 (0.863, 1.282)	0.617	NA	NA
CDRS	2.081 (1.045, 4.144)	0.037*	2.104 (1.126,3.935)	0.02*
ADAS	1.18 (1.043, 1.335)	0.009*	1.244 (1.109,1.396)	< 0.001*
MMSE	0.841 (0.618, 1.144)	0.27	NA	NA
SVM score	1.439 (1.114, 1.808)	< 0.001*	1.144 (0.726, 1.802)	< 0.001*

OR Odds ratio, *CI* Confidence interval, *CDRS* Clinical Dementia Rating Scale, *ADAS* Alzheimer's Disease Assessment Scale, *MMSE* Mini-Mental State Examination, *SVM* Support vector machine, *NA* Not available because the variable is not included in multiple variables

structural changes in multiple brain regions. Detecting these changes may facilitate new screening strategies to identify additional essential targets. Therefore, the DTI and network features in these important areas can be used as imaging indicators to assist in diagnosing and evaluating AD [33, 34].

To further improve the performance of the model, CDRS and ADAS were also included in this study, both of which are widely used in the assessment of cognitive change in clinical trials, and Wessels AM [35] found that ADAS-Cog appeared to be more valuable than CDR-SB in detecting differences in treatment groups. The diagnostic performance of ADAS in predicting MCI disease progression was higher than that of CDRS in this study, reflecting the higher accuracy of ADAS in cognitive change. However, in this study, there was no difference in MCI between the stable and progressive groups of APOE4 in the test group. We speculate that this may be due to two reasons: firstly, the imbalanced distribution of data; Secondly, its effect on the chronic process of disease progression is not as significant as that of the disease itself. The novelty of the present study lies in the extracted series of features related to white matter. There have been similar studies of the cerebral cortex. For example, Gupta et al. used this method to study the cortex, subcortical, and hippocampal regions and achieved a classification effect of 0.9333 for MCI progression [36]. We obtained similar results. However, while Gupta et al. focused on a 2-year transition, we conducted a 4-year follow-up observational study. Moreover, we additionally considered features of the white matter network. Therefore, the proposed white matter-derived model

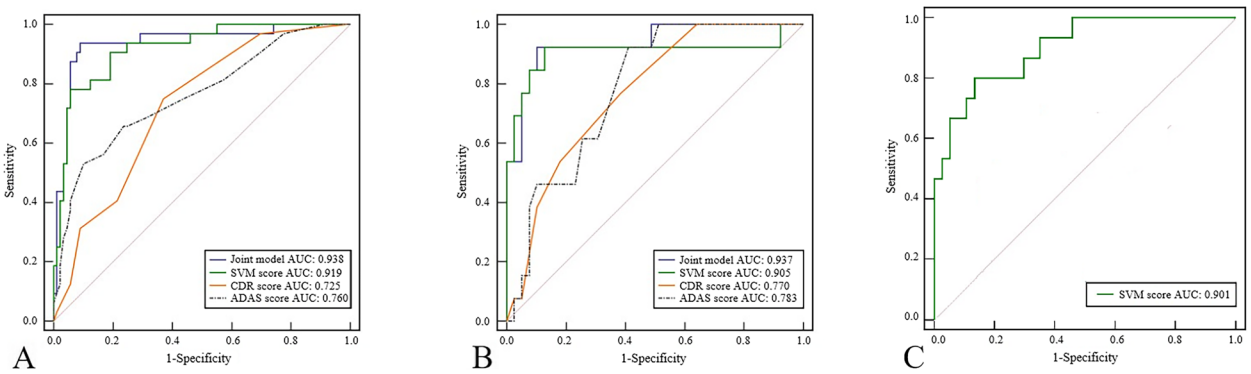

Fig. 5 **A** and **B** show the diagnostic performance of the joint model and individual predictors in the training and testing cohorts. **C** shows the diagnostic performance of the SVM score model in the validation group

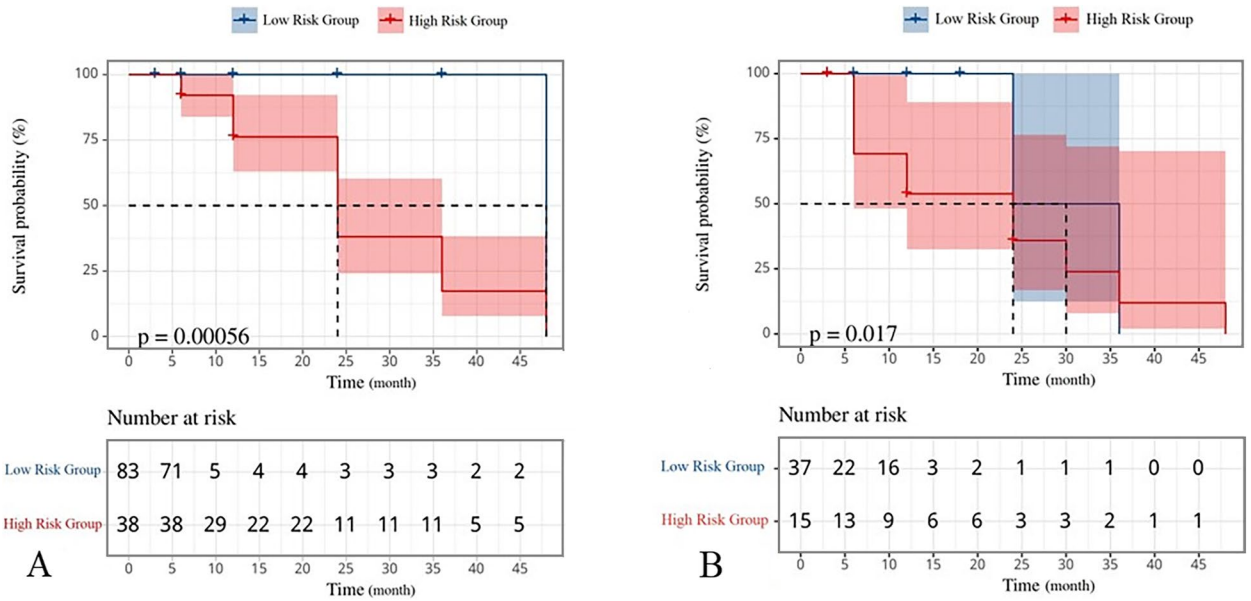

Fig. 6 **A** and **B** show significant differences in the Survival curve analysis of the low-risk and high-risk groups classified by the joint model in the training and testing group ($p < 0.05$)

may be more suitable for long-term follow-up observations and proves the critical impact of white matter on cognitive impairment [37, 38]. In particular, our results support that DTI and brain network features of essential regions in the brain can be used as auxiliary imaging indicators for diagnosing and evaluating AD cases.

There were limitations associated with this study. First, as a retrospective study, the simulation of retrospective statistics may have depended on too many assumptions. Secondly, further optimization of the prediction model is needed through better engineering design. A more comprehensive integration of other clinical data may improve the model's performance. In addition, the higher the interpretability of machine learning models, the easier it is for people to understand why certain decisions or predictions are made. In the future, we will incorporate machine learning interpretability methods such as Shapley additive explanation (SHAP) and local interpretable model-agnostic explanations (LIME) to enrich the models [39].

In summary, extracting multiple-dimensional features from white matter provides supplementary information regarding the progression of MCI. Furthermore, by combining novel white matter features and clinical scores to build a prediction model, we can effectively and robustly identify individuals who are high-risk MCI patients. It is anticipated that this approach can facilitate the diagnosis of AD at an earlier stage.

Abbreviations

MCI	Mild cognitive impairment
AD	Alzheimer's disease
DTI	Diffusion tensor imaging
MRI	Magnetic resonance imaging
FA	Fractional anisotropy
MD	Mean diffusivity
rAD	Axial diffusion
RD	Radial diffusion
MMSE	Mini-mental state examination
CDR	Clinical dementia rating
ADAS	Alzheimer's disease assessment scale
mRMR	Max-relevance and min-redundancy
LASSO	Least absolute shrinkage and selection operator
GBDT	Gradient boosting decision tree
SD	Standard deviation
RSD	Relative standard deviation
AIC	Akaike information criterion
OR	Odds ratio
PI	Prognostic index
SVM	Support vector machine
NB	Naive bayes
DT	Decision tree
RF	Random forest
KNN	K-nearest neighbors
MCP	Middle cerebellar peduncle
HCB	Hippocampal cingulum bundle
BC	Betweenness centrality
SHAP	Shapley additive explanation
LIME	Local interpretable model-agnostic explanations

Supplementary Information

The online version contains supplementary material available at https://doi.org/10.1186/s12877-024-05293-7.

Supplementary Material 1

Acknowledgements

Data collection and sharing for this project were funded by the Alzheimer's Disease Neuroimaging Initiative (ADNI) (National Institutes of Health Grant U01 AG024904) . ADNI is funded by the National Institute on Aging, the National Institute of Biomedical Imaging and Bioengineering, and through generous contributions from the following: AbbVie, Alzheimer's Association; Alzheimer's Drug Discovery Foundation; Araclon Biotech; BioClinica, Inc.; Biogen; Bristol-Myers Squibb Company; CereSpir, Inc.; Cogstate; Eisai Inc.; Elan Pharmaceuticals, Inc.; Eli Lilly and Company; EuroImmun; F. Hoffmann-La Roche Ltd and its affiliated company Genentech, Inc.; Fujirebio; GE Healthcare; IXICO Ltd.; Janssen Alzheimer Immunotherapy Research & Development, LLC.; Johnson & Johnson Pharmaceutical Research & Development LLC.; Lumosity; Lundbeck; Merck & Co., Inc.; Meso Scale Diagnostics, LLC.; NeuroRx Research; Neurotrack Technologies; Novartis Pharmaceuticals Corporation; Pfizer Inc.; Piramal Imaging; Servier; Takeda Pharmaceutical Company; and Transition Therapeutics. The Canadian Institutes of Health Research is providing funds to support ADNI clinical sites in Canada. Private sector contributions are facilitated by the Foundation for the National Institutes of Health (www.fnih.org). The grantee organization is the Northern California Institute for Research and Education, and the study is coordinated by the Alzheimer's Therapeutic Research Institute at the University of Southern California. ADNI data are disseminated by the Laboratory for Neuro Imaging at the University of Southern California.

Authors' contributions

Zhenyu Shu, Jiaxuan Peng, and Guangying Zheng contributed to the conception and design of the study. Mengmeng Hu, Zihan Zhang, and Zhongyu Yuan provided and prepared the samples. Yuyun Xu, Yuan Shao, and Yang Zhang reconstructed and analyzed the images. Xiaojun Sun, Lu Han, and Xiaokai Gu analyzed and interpreted the data. Zhenyu Shu wrote the manuscript with input from all authors.

Funding

The work was supported by the National Natural Science Foundation of China (Grant No. 82101983), the Health Commission of Zhejiang Province(2022KY556) and the Zhejiang Provincial Natural Science Foundation of China(LGF22H090021).

Availability of data and materials

Data used in the preparation of this article were obtained from the Alzheimer's Disease Neuroimaging Initiative (ADNI) database (adni.loni.usc.edu) and the NACC database (https://naccdata.org). As such, the investigators within the ADNI contributed to the design and implementation of ADNI and/or provided data but did not participate in the analysis or writing of this report. A complete listing of ADNI investigators can be found at: https://adni.loni.usc.edu/wp-content/ADNI-Acknowledgement-List.pdf. The data that support the findings of this study are available from ADNI but restrictions apply to the availability of these data, which were used under license for the current study, and so are not publicly available. Data can be accessed through application to ADNI database (https://adni.loni.usc.edu/data-samples/adni-data/).

Declarations

Ethics approval and consent to participate

The present study was approved and granted permission to access the public data of the ADNI database (https://adni.loni.usc.edu/) and the NACC database (https://naccdata.org). As such, the investigators within the ADNI contributed to the design and implementation of ADNI and provided data but did not participate in the analysis or writing of this report. A complete listing of ADNI investigators can be found at: https://adni.loni.usc.edu/data-samples/access-data/

Consent for publication

Not applicable.

Competing interests

The authors declare no competing interests.

Author details

[1]Center for Rehabilitation Medicine, Department of Radiology, Zhejiang Provincial People's Hospital (Affiliated People's Hospital, Hangzhou Medical College), Hangzhou, Zhejiang, China. [2]Jinzhou Medical University, Jinzhou, Liaoning Province, China. [3]Zhejiang University of Technology, Zhejiang Province, Hangzhou, China.

Received: 23 June 2023 Accepted: 8 August 2024
Published online: 19 August 2024

References

1. Satizabal CL, Beiser AS, Chouraki V, et al. Incidence of dementia over three decades in the framingham heart study. N Engl J Med. 2016;374(6):523–32.
2. Janoutová J, Šerý O, Hosák L, Janout V. Is mild cognitive impairment a precursor of Alzheimer's disease? Short review. Cent Eur J Public Health. 2015;23(4):365–7.
3. Langa KM, Levine DA. The diagnosis and management of mild cognitive impairment: a clinical review. JAMA. 2014;312(23):2551–61.
4. Parvizi J. Corticocentric myopia: old bias in new cognitive sciences. Trends Cogn Sci. 2009;13(8):354–9.
5. Catani M, Dell'acqua F, Bizzi A, et al. Beyond cortical localization in clinico-anatomical correlation. Cortex. 2012;48(10):1262–87.
6. Scheib J, Höke A. Advances in peripheral nerve regeneration. Nat Rev Neurol. 2013;9(12):668–76.
7. Delbeuck X, Van der Linden M, Collette F. Alzheimer's disease as a disconnection syndrome? Neuropsychol Rev. 2003;13(2):79–92.
8. Prescott JW, Doraiswamy PM, Gamberger D, et al. Diffusion Tensor MRI structural connectivity and PET amyloid burden in preclinical autosomal dominant alzheimer disease: the DIAN Cohort. Radiology. 2022;302(1):143–50.

9. Zhang J, Aggarwal M, Mori S. Structural insights into the rodent CNS via diffusion tensor imaging. Trends Neurosci. 2012;35(7):412–21.
10. Filley CM. White matter and behavioral neurology. Ann N Y Acad Sci. 2005;1064:162–83.
11. Mihaescu AS, Kim J, Masellis M, et al. Graph theory analysis of the dopamine D2 receptor network in Parkinson's disease patients with cognitive decline. J Neurosci Res. 2021;99(3):947–65.
12. delEtoile J, Adeli H. Graph theory and brain connectivity in Alzheimer's disease. Neuroscientist. 2017;23(6):616–26.
13. Jordan MI, Mitchell TM. Machine learning: trends, perspectives, and prospects. Science. 2015;349(6245):255–60.
14. Battista P, Salvatore C, Berlingeri M, et al. Artificial intelligence and neuropsychological measures: the case of Alzheimer's disease. Neurosci Biobehav Rev. 2020;114:211–28.
15. Morris JC. The Clinical Dementia Rating (CDR): current version and scoring rules. Neurology. 1993;43(11):2412–4. https://doi.org/10.1212/wnl.43.11.2412-a. PMID: 8232972.
16. Mori S, Oishi K, Jiang H, et al. Stereotaxic white matter atlas based on diffusion tensor imaging in an ICBM template. Neuroimage. 2008;40(2):570–82.
17. Oishi K, Zilles K, Amunts K, et al. Human brain white matter atlas: identification and assignment of common anatomical structures in superficial white matter. Neuroimage. 2008;43(3):447–57.
18. Dziak JJ, Coffman DL, Lanza ST, et al. Sensitivity and specificity of information criteria. Brief Bioinform. 2020;21(2):553–65.
19. Bergamino M, Keeling EG, Mishra VR, et al. Assessing white matter pathology in early-stage parkinson disease using diffusion MRI: a systematic review. Front Neurol. 2020;11: 314.
20. Hiyoshi-Taniguchi K, Oishi N, Namiki C, et al. The uncinate fasciculus as a predictor of conversion from amnestic mild cognitive impairment to Alzheimer disease. J Neuroimaging. 2015;25(5):748–53.
21. Bozzali M, Giulietti G, Basile B, et al. Damage to the cingulum contributes to Alzheimer's disease pathophysiology by deafferentation mechanism. Hum Brain Mapp. 2012;33(6):1295–308.
22. Zhao K, Ding Y, Han Y, et al. Independent and reproducible hippocampal radiomic biomarkers for multisite Alzheimer's disease: diagnosis, longitudinal progress and biological basis. Sci Bull (Beijing). 2020;65(13):1103–13.
23. Murray AN, Chandler HL, Lancaster TM. Multimodal hippocampal and amygdala subfield volumetry in polygenic risk for Alzheimer's disease. Neurobiol Aging. 2021;98:33–41.
24. Rudebeck SR, Scholz J, Millington R, et al. Fornix microstructure correlates with recollection but not familiarity memory. J Neurosci. 2009;29(47):14987–92.
25. Fletcher E, Raman M, Huebner P, et al. Loss of fornix white matter volume as a predictor of cognitive impairment in cognitively normal elderly individuals. JAMA Neurol. 2013;70(11):1389–95.
26. Gupta V, Booth S, Ko JH. Hypermetabolic cerebellar connectome in Alzheimer's disease. Brain Connect. 2021;13(6):356–66.
27. Stone DB, Ryman SG, Hartman AP, et al. Specific white matter tracts and diffusion properties predict conversion from mild cognitive impairment to Alzheimer's disease. Front Aging Neurosci. 2021;13:711579.
28. Douaud G, Menke RA, Gass A, et al. Brain microstructure reveals early abnormalities more than two years prior to clinical progression from mild cognitive impairment to Alzheimer's disease. J Neurosci. 2013;33(5):2147–55.
29. Gong Y, Zhang Z. Global robustness and identifiability of random, scale-free, and small-world networks. Ann N Y Acad Sci. 2009;1158:82–92.
30. Zhang T, Liao Q, Zhang D, et al. Predicting MCI to AD Conversation Using Integrated sMRI and rs-fMRI: Machine Learning and Graph Theory Approach. Front Aging Neurosci. 2021;13: 688926.
31. Hojjati SH, Ebrahimzadeh A, Khazaee A, et al. Predicting conversion from MCI to AD using resting-state fMRI, graph theoretical approach and SVM. J Neurosci Methods. 2017;282:69–80.
32. Zhou Y, Si X, Chen Y, Chao Y, et al. Hippocampus- and thalamus-related fiber-specific white matter reductions in mild cognitive impairment. Cereb Cortex. 2022;32(15):3159–74.
33. Cano SJ, Posner HB, Moline ML, et al. The ADAS-cog in Alzheimer's disease clinical trials: psychometric evaluation of the sum and its parts. J Neurol Neurosurg Psychiatry. 2010D;81(12):1363–8.
34. Hughes CP, Berg L, Danziger WL, et al. A new clinical scale for the staging of dementia. Br J Psychiatry. 1982;140:566–72. https://doi.org/10.1192/bjp.140.6.566. PMID: 7104545.
35. Wessels AM, Dowsett SA, Sims JR. Detecting treatment group differences in alzheimer's disease clinical trials: a comparison of Alzheimer's Disease Assessment Scale - Cognitive Subscale (ADAS-Cog) and the Clinical Dementia Rating - Sum of Boxes (CDR-SB). J Prev Alzheimers Dis. 2018;5(1):15–20. https://doi.org/10.14283/jpad.2018.2. PMID: 29405227.
36. Gupta Y, Lee KH, Choi KY, et al. Early diagnosis of Alzheimer's disease using combined features from voxel-based morphometry and cortical, subcortical, and hippocampus regions of MRI T1 brain images. PLoS ONE. 2019;14(10):e0222446.
37. Wen Q, Mustafi SM, Li J, et al. White matter alterations in early-stage Alzheimer's disease: a tract-specific study. Alzheimers Dement (Amst). 2019;11:576–87.
38. Coelho A, Fernandes HM, Magalhães R, et al. Signatures of white-matter microstructure degradation during aging and its association with cognitive status. Sci Rep. 2021;11(1):4517.
39. Alabi RO, Elmusrati M, Leivo I, et al. Machine learning explainability in nasopharyngeal cancer survival using LIME and SHAP. Sci Rep. 2023;13(1):8984. https://doi.org/10.1038/s41598-023-35795-0. PMID:37268685;PMCID:PMC10238539.

Publisher's Note